Materials Today: Proceedings xxx (xxxx) xxx

Contents lists available at ScienceDirect

Materials Today: Proceedings

journal homepage: www.elsevier.com/locate/matpr

# Effect of post weld heat treatments on microstructure and mechanical properties of dissimilar P92 steel-AISI 304H ASS A-TIG weld joint

Pratishtha Sharma [a,*], Dheerendra Kumar Dwivedi [b], Gaurav Sharma [c]

[a] Mechanical Engineering Department, ABES Engineering College, Ghaziabad, Uttar Pradesh 201009, India
[b] Department of Mechanical and Industrial Engineering, Indian Institute of Technology Roorkee, Uttarakhand 247667, India
[c] Mechanical Engineering Department, KIET Group of Institutions, Delhi-NCR, Ghaziabad 201206, India

ARTICLE INFO

*Keywords:*
A-TIG welding
P92 steel
Post weld heat treatment
Microstructure
Mechanical properties

ABSTRACT

In present work, the efficacy of post weld heat treatment (PWHT) on microstructure and mechanical properties of dissimilar P92 steel-AISI 304H austenitic stainless steel (ASS) activated flux-tungsten inert gas (A-TIG) weld joint was studied. Based on the time temperature cycle, the post weld heat treatment was performed in two ways: (a) PWHT-1 (760 °C, 2 h) and (b) PWHT-2 (1160 °C, 2 h and 760 °C, 2 h). After PWHTs, the microstructure and mechanical properties (micro-hardness, tensile behavior and impact toughness) of weld joint were tested and compared with as-welded condition. PWHT-1 resulted in coarsening of existing precipitates and formation of new precipitates in weld zone. The average size of precipitates along the PAGB and inside the grain matrix was measured to be 294 ± 50 nm and 153 ± 50 nm, respectively. After PWHT-2, the microstructure of P92 FGHAZ, P92 CGHAZ and weld zone were observed to be quite similar due to the re- austenitisation during this PWHT regime. The hardness distribution shows the non-uniformity even after PWHT-1 however; PWHT-2 shows negligible variation in hardness of P92 side HAZs and weld zone. In tensile testing, the failure location has been changed to P92 steel base metal from AISI 304H ASS which suggests that P92 steel becomes weak after the post weld heat treatments. An increase in elongation % (PWHT-1: 37% and PWHT-2: 45%) was also obtained after PWHTs. Upon PWHTs the weld zone impact toughness also improved (PWHT-1: 59 ± 2 J and PWHT-2: 132 ± 2 J) and satisfy the minimum average impact toughness as per standard EN 1559:1999.

## 1. Introduction

To meet the high demand of power generation, the heat conversion units of thermal power plants utilize the materials with better mechanical properties. P92 steel is considered as an appropriate material for steam headers and pipes in thermal power plants due to the low thermal expansion coefficient, high oxidation resistance, high thermal conductivity and creep strength [1]. This class of steel is mainly used for fabrication of components where the operating temperature and pressure are in range of 580 °C–625 °C and 250 bar–300 bar, respectively. The P92 steel was developed to improve the creep strength of P91 steel especially at high temperature by addition of alloying element like 1.5% W, 0.005% B and reducing the Mo content to 0.5%. On the other hand, the AISI 304H steel belongs to austenitic stainless steel (ASS) group. The ASS is mainly used in construction of economizer, pre-heaters and superheaters due to good high-temperature creep resistance and corrosion [2]. Therefore, the joining of P92 steel and AISI 304H ASS is rather necessary and the integrity of this joint plays a crucial role in operation of thermal power plants. In published literature, researchers have attempted to develop the welding process for joining of such type of dissimilar metal combination [3–7]. The mechanical properties of such dissimilar weld joint have been reported poor and not as per the required standards. Some of the recent works reported the various methods of improving the mechanical properties of these joints such as insertion of interlayers [6] and external wire feeding [8].

However, these methods are base metal dependent and need rigorous initial efforts to develop the process. Therefore, the PWHT is the most conventional and easy way to improve the mechanical properties of weld joints. In published literature, few researchers have reported the effect of PWHT on similar P91/P92 steel weld joint and the dissimilar weld joint obtained using various filler wires in Multipass-TIG welding. Arivazhagan et al. [9] studied the effect of PWHT on microstructure and mechanical properties of P91 weld joint and reported that the minimum toughness value was observed for Weld zone and maximum for CGHAZ.

* Corresponding author.
*E-mail address:* pratishtha@abes.ac.in (P. Sharma).

https://doi.org/10.1016/j.matpr.2023.08.327
Received 3 July 2023; Received in revised form 21 August 2023; Accepted 27 August 2023

**Table 1**
Chemical composition of base metals P92 steel and AISI 304H ASS.

| | C | Si | Mn | Cr | Mo | Ni | Nb | V | W | Cu | Fe |
|---|---|---|---|---|---|---|---|---|---|---|---|
| **P92 steel** | 0.09 | 0.11 | 0.39 | 8.94 | 0.41 | 0.18 | 0.06 | 0.18 | 1.59 | – | Bal. |
| **AISI 304H ASS** | 0.10 | 0.22 | 1.65 | 18.38 | 0.22 | 8.57 | 0.16 | – | – | 0.23 | |

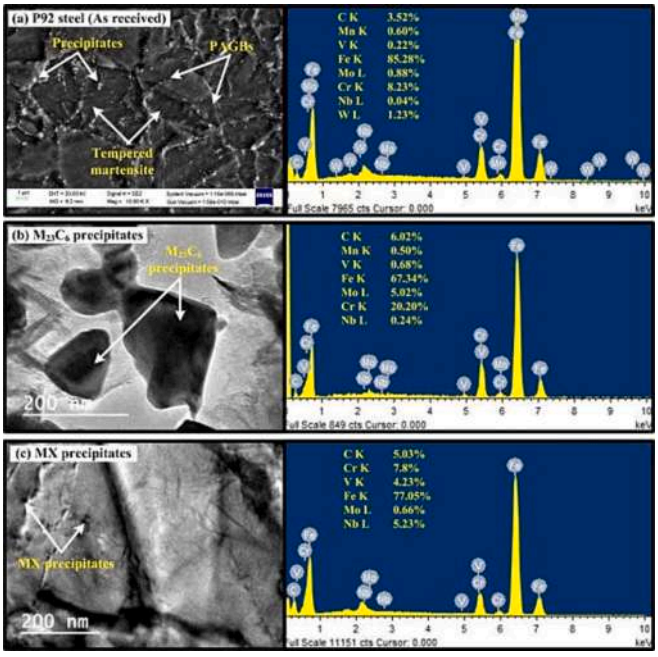


**Fig. 1.** FE-SEM micrographs and EDS spectrum of base metals: (a) as received P92 steel, (b) $M_{23}C_6$ secondary particles, and (c) MX secondary particles.

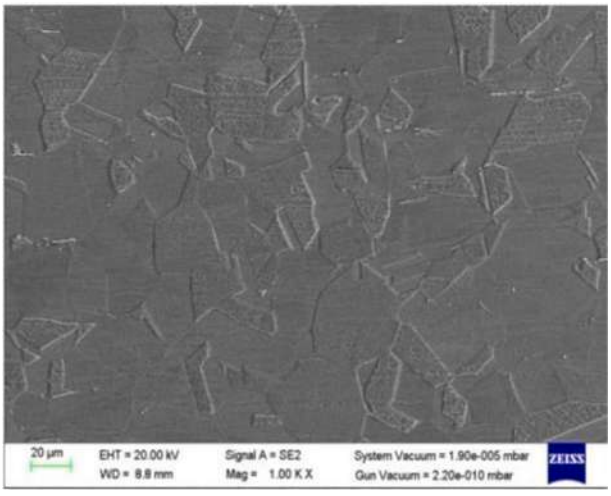


**Fig. 2.** FE-SEM micrograph of AISI 304H ASS.

Saini et al. [10] studied the effect of post weld normalizing and tempering (PWNT) on microstructure characteristics and mechanical behavior of ferritic- martensitic steel weld joint and found that the superior microstructure and mechanical properties after PWNT. Pandey et al. [11] had also compared the microstructure and mechanical properties of gas tungsten arc welded P91 steel joints and found the PWNT joint as superior. A lot of work is published on the effect of PWHT on similar weld joint However; the studies related to the effect of PWHT on microstructure and mechanical properties on dissimilar weld joint are scarce. The studies of PWHT are comparatively complex due to heterogeneous microstructure. Also, in the published works the PWHT parameters time and temperature are conventional and mostly based on filler material and ferritic/martensitic steel. The heterogeneous microstructure of weld joint makes the selection of PWHT parameters i.e. time and temperature even more complex. In present work, attempts have been made to study the effect of two different post weld heat treatments named as PWHT-1 (760 °C, 2 h) and PWHT-2 (1160 °C, 2 h and 760 °C, 2 h) and a relationship was developed between microstructure and mechanical properties.

**Table 2**
Mechanical properties of as received P92 steel base metal and 304H ASS base metal.

| | P92 steel base metal | 304H ASS base metal |
|---|---|---|
| **Hardness (HV)** | 202.4 | 173.3 |
| **Ultimate tensile strength (MPa)** | 755.2 | 685.8 |
| **Yield strength (MPa)** | 490.5 | 364.5 |
| **Elongation (%)** | 23.6 | 79.2 |
| **Impact toughness (J)** | 82 ± 2 | 132 ± 2 |

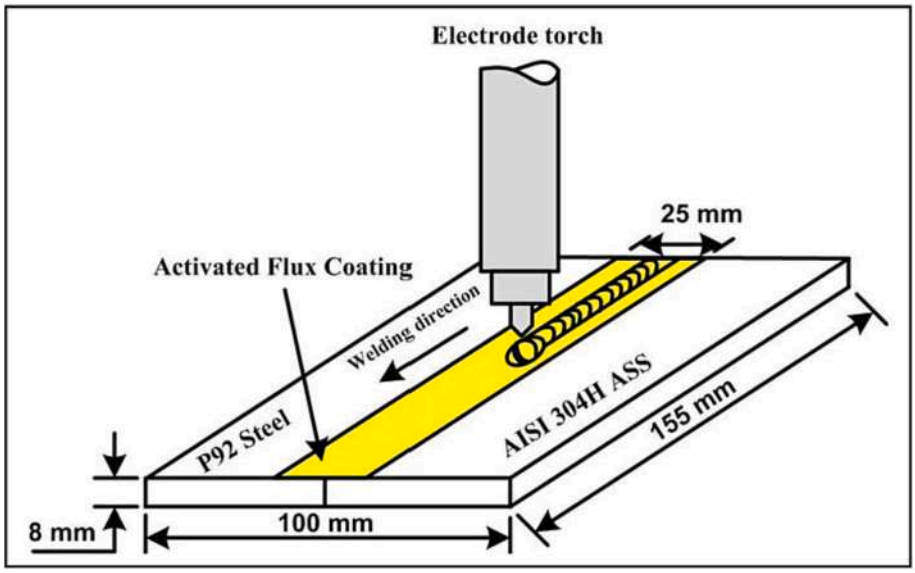


**Fig. 3.** Schematic of coating pattern and torch position for dissimilar weld formation of P92 steel-AISI 304H ASS developed using A-TIG welding.

## 2. Experimental details

### 2.1. Materials

In this work, two different steels (P92 steel and AISI 304H ASS) were used. The elemental composition of the as received (Normalized and tempered) P92 steel is given in Table 1. The microstructure of P92 steel predominantly exhibited lath martensitic structure (Fig. 1 a) and the prior austenite grain boundaries (PAGBs) were also visible. Few precipitates were also distributed inside the grain matrix and in the lath region. To measure the size of precipitates, transmission electron microscopy (TEM) images at high magnification are presented in Fig. 1 b. Fine precipitates of average size 32 ± 25 nm were distributed inside the grain matrix and coarse precipitates of average size 210 ± 80 nm were decorated along the PAGBs (Fig. 1 a, b). The energy dispersive spectroscopy (EDS) suggested that precipitates inside the grain matrix were enriched with Nb, V, C and N (can be MX type) and the precipitates distributed along the PAGBs were enriched with Fe, Cr, Mo and C (can be M23C6 type) (Fig. 1 c, d). The elemental composition of the AISI 304H ASS base metal is also presented in Table 1. The microstructure (Fig. 2) showed the polygonal equiaxed austenitic grain structure with parallel twins.

The mechanical properties of both the base metals (in as-received condition) are given in Table 2. The P92 steel base metal was supplied in normalized (at 1050 °C for 1 h) and tempered (at 750 °C for 1 h) condition, whereas; 304H ASS was supplied in annealed condition. Both the materials were purchased from M/s Nextgen Steels and Alloys, Mumbai, India. The mechanical properties, supply status and manufacturer of the base metals have been included in revised manuscript.

For macrostructure and microstructure studies, the cut samples were cut and etched using following etchants: (a) P92 steel Villela's reagent (1 g Picric acid+ 5 ml HCl + 100 ml Ethanol) and (b) AISI 304H ASS Electrochemical etching at 9 V in (10% oxalic acid + 90% distilled water solution).

## 3. Welding process

The schematic of welding set-up for A-TIG welding is presented in Fig. 3. Both the base metal plates were first cut and shaped into rectangular shape (155 mm × 50 mm × 8 mm). Then after, finished plates were tack welded with no root gap and then coating of flux paste ($TiO_2$ + acetone) was performed using a paint brush. Flux coated plates were left in the environment till the acetone gets evaporate fully. Afterwards, welding was performed using a TIG welding machine (semiautomatic) with the process parameters (Welding current: 220 A, Average arc voltage: 14.56 V and arc length: 3 mm).

### 3.1. Post weld heat treatment

In present work, the PWHT was performed in two ways: (a) PWHT-1 and (b) PWHT-2. The schematic representation showing the temperature–time variation for both the PWHTs is shown in Fig. 4. In literature [10,12,13], it is suggested that the heat treatment temperature should be below the lower critical temperature ($AC_1$) to improve impact toughness and ductility of weld joint. For P92 steel, the $AC_1$ temperature is 876 °C. Therefore, in PWHT-1 the samples were heated at 760 °C for 2 h soaking time then after samples were left in ambient to cool. After PWHT-1, it was found that the distribution of precipitate was non homogeneous across the weld zone and P92 steel side HAZs. The microhardness was also non-uniform. Therefore, the PWHT-2 was carried out. The PWHT-2 comprises two time temperature cycles. In first cycle, the samples were heated above upper critical temperature ($A_{c3}$) at 1160 °C for 2 h soaking time then after samples were left in ambient to cool till the room temperature is achieved. Thereafter, the samples were subjected to second cycle i.e. samples were heated at 760 °C for 2 h soaking time followed by air cooling. The purpose of selection of time-temperature cycle in PWHT-2 is to homogenize the microstructure of HAZs of weld joint.

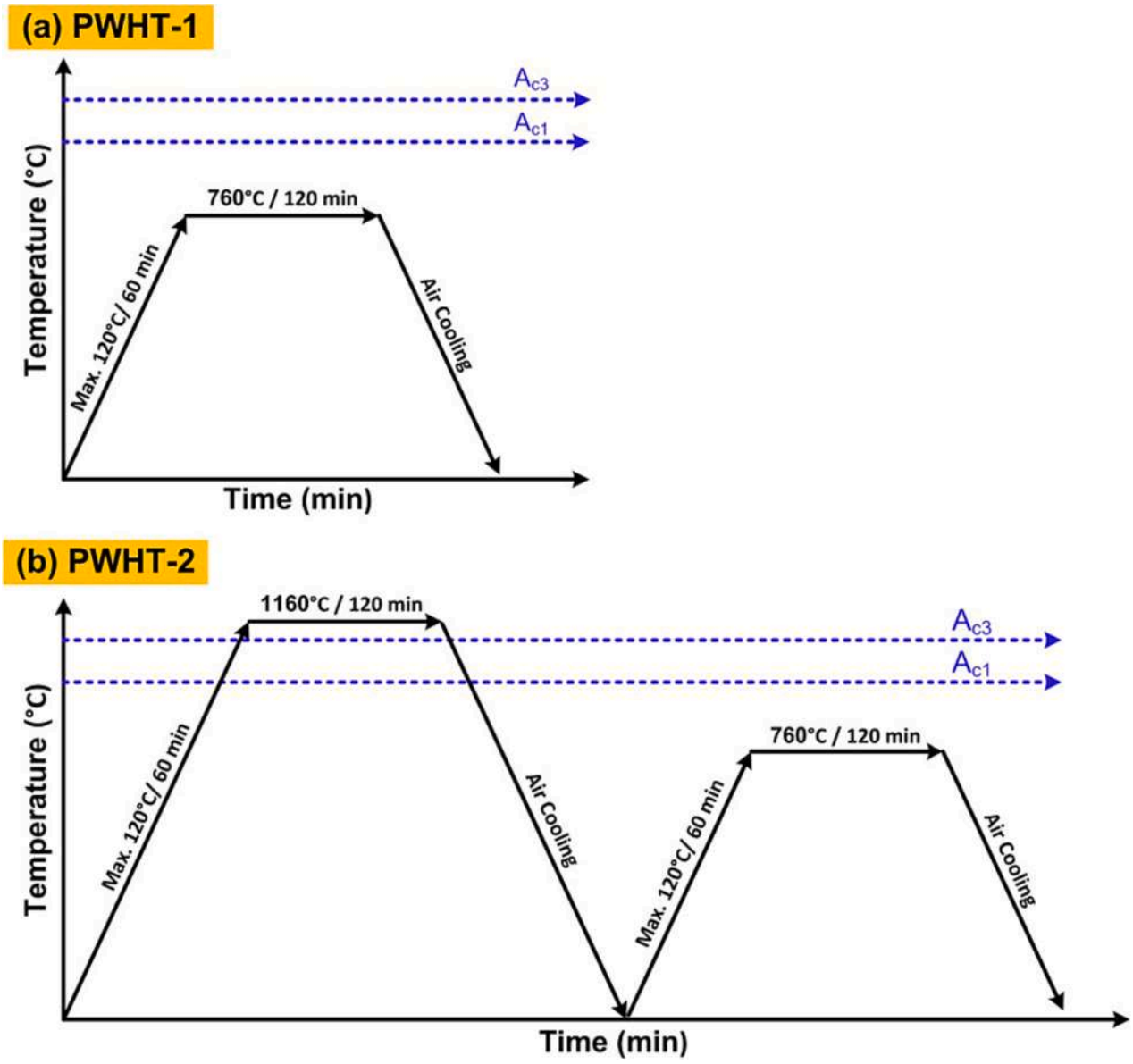


**Fig. 4.** Schematic representation of temperature–time variation for (a) PWHT-1 and (b) PWHT-2.

## 4. Results and discussion

### 4.1. Microstructure study

The FE-SEM micrographs of P92 FGHAZ, P92 CGHAZ and weld zone after PWHT-1 and PWHT-2 are shown in Fig. 5. After PWHT-1, the CGHAZ and FGHAZ show tempered lath martensitic structure. PWHT-1 resulted in the precipitation of globular $M_{23}C_6$ precipitates and precipitates (fine V/Nb rich MX type) in the CGHAZ of size 220 ± 50 nm. In FGHAZ, the PWHT-1 coarsened the existing precipitates and formed the new precipitates. The average size of precipitates along the PAGB and inside the grain matrix was measured to be 294 ± 50 nm and 153 ± 50 nm, respectively. Cao et al. [14] also reported the coarsening of precipitates HAZs and base metal in P92 steel after PWHT. After PWHT-2, the microstructure of P92 FGHAZ, P92 CGHAZ and weld zone were observed to be quite similar. This could be due to the re- austenitisation during this PWHT regime. The re-austenitisation resulted in the untempered martensite in each zone and full dissolution of precipitates into the main matrix [15]. The re-austenitized samples were subjected to second cycle i.e. heating at 760 °C tailed by air cooling. During second cycle, the tempering of untempered martensite took place which resulted in formation in tempered martensitic structure. The precipitates were also distributed along the PAGBs.

## 5. Mechanical properties

### 5.1. Micro-hardness distribution

The micro-hardness profile of A-TIG weld joint in various conditions is shown in Fig. 6. The PWHT-1 results in the substantial reduction in hardness of P92 side HAZs and weld zone as compared to as-welded condition. The average hardness (HV) of P92 FGHAZ, P92 CGHAZ and weld zone was measured to be 221, 311 and 269, respectively. Softening of martensite leads to the dislocation annihilation which in turn resulted in lowering of hardness values [16], martensite tempering and reduction in solid solution strengthening elements in the metal matrix due to the formation of fresh $M_{23}C_6$ and MX precipitates. The hardness of AISI 304H ASS HAZ/base is less affected by PWHT-1. It is also observed that the heterogeneity across the transverse section of weld joint still remain even after PWHT-1. The micro-hardness distribution curve after PWHT-

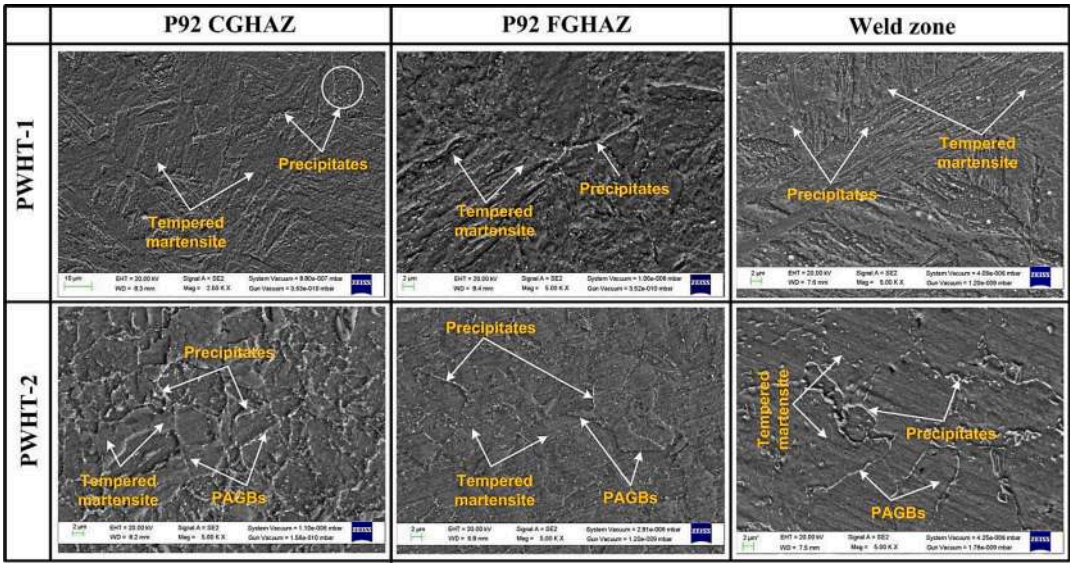


**Fig. 5.** The FE-SEM micrographs of P92 CGHAZ, P92 FGHAZ and weld zone of dissimilar P92 steel-AISI 304H ASS A-TIG weld joint in: (a) after PWHT-1 and (b) PWHT-2.

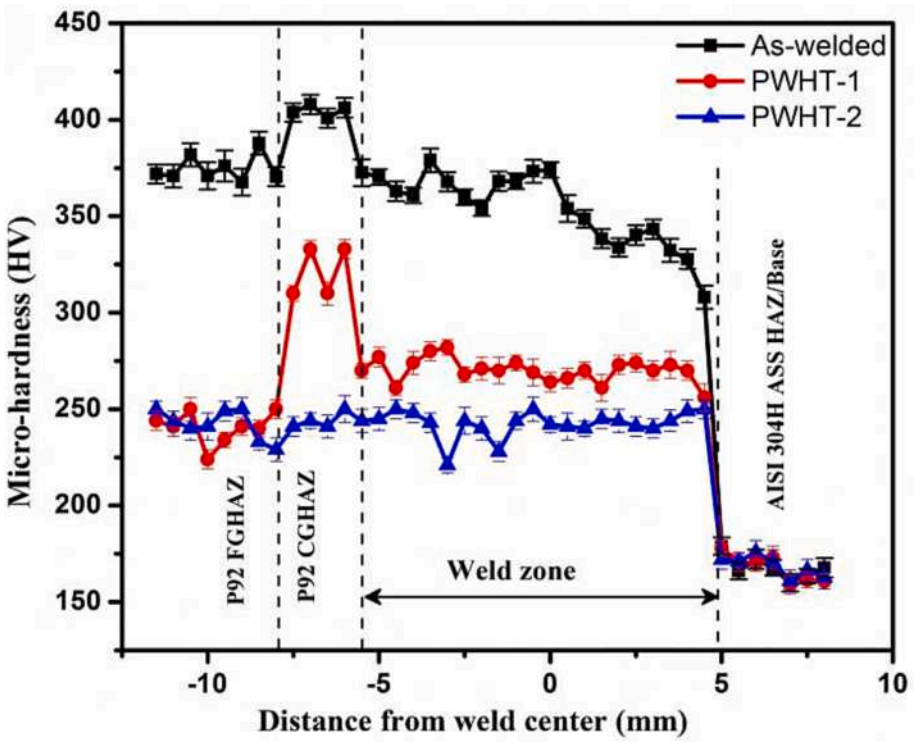


**Fig. 6.** Micro-hardness distribution curves for A-TIG weld joint of dissimilar P92 steel-AISI 304H ASS in as-welded condition, after PWHT-1 and PWHT-2.

2 shows almost negligible variation at P92 side and weld zone. The average hardness (HV) of P92 FGHAZ, P92 CGHAZ and weld zone was measured to be 231, 240 and 242, respectively. However, the average hardness of AISI 304H ASS HAZ/base metal is still remain unaffected and measured to be 172 and 161, respectively.

*5.1.1. Tensile testing*

Tensile testing was performed to study the efficacy of PWHTs on tensile properties (ultimate tensile strength (UTS), yield strength (YS) and elongation %). The tensile test sample after failure are shown in Fig. 7. It can be seen that the tensile test in as-welded condition failed from AISI 304H ASS base metal. Upon PWHT-1 and PWHT-2, the failure location has been changed to P92 steel base metal which suggests that P92 steel becomes weak after the post weld heat treatments. Cao et al. [17], have suggested that in 9–12% Cr martensitic steel the lath-substructure strengthening is the major strengthening mechanism. However, after PWHT-1 and PWHT-2 no martensite laths were detected in P92 steel base metal, therefore, it actually becomes a soft zone and failure took place form this zone under tensile loading. The stress–strain curve were plotted and given in Fig. 8. After PWHT-1 and PWHT-2, the UTS was obtained to be 680 MPa and 669 MPa, respectively which is comparable to that in as-welded condition In as-welded condition (688

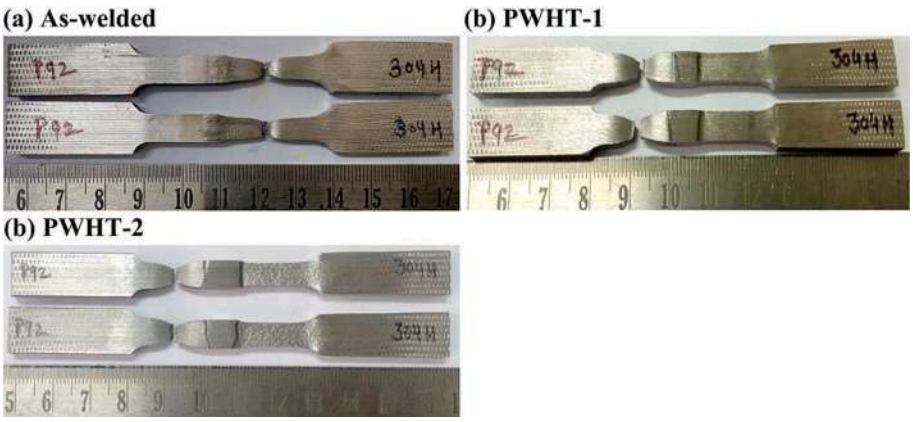


**Fig. 7.** Photographs of tensile test specimens after test: (a) in as-welded condition, (b) after PWHT-1 and (c) after PWHT-2.

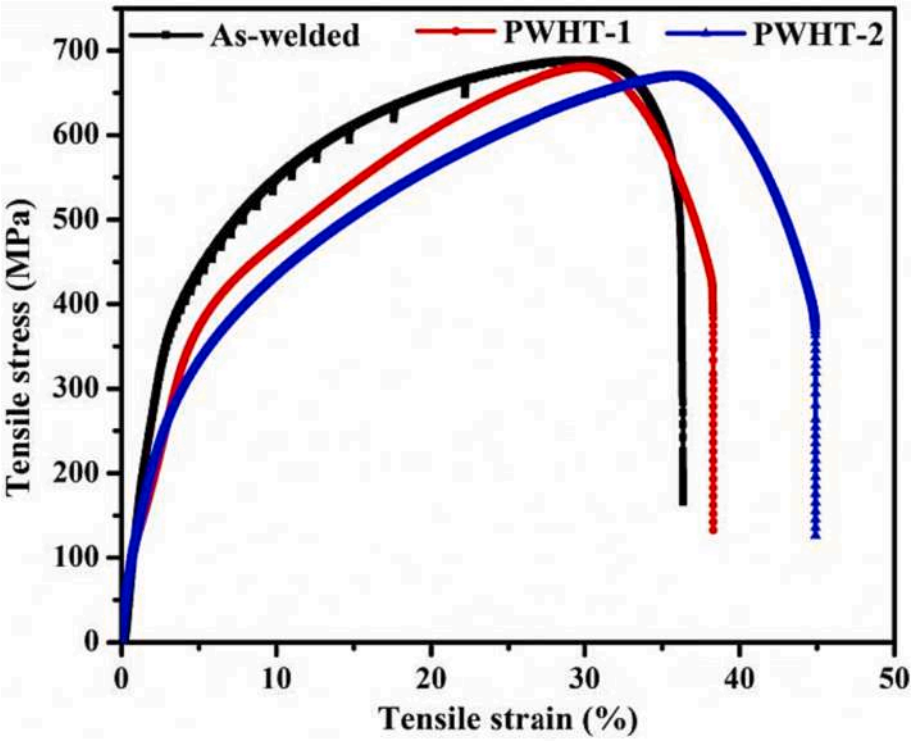


**Fig. 8.** Tensile stress–strain curve for the weld joints in as-welded and PWHT condition.

MPa). The strength of weld joint in PWHT-1 and PWHT-2 were corresponding to the strength of P92 steel base metal. The elongation % of as-welded joint was obtained to be as 37%. Upon PWHT-1, the weld joint showed the slight improvement (38%) in ductility which could be due to the tempering of weld zone, P92 steel HAZ/base metal. Upon PWHT-2, the highest value of ductility (45%) was observed.

*5.1.2. V-notch Charpy impact toughness testing*

To study the efficacy of PWHTs on impact toughness of weld zone, the V-notch Charpy impact toughness test was conducted. After test, the impact toughness samples are shown in Fig. 9. The as-welded joint showed the poor impact toughness (30 ± 2 J). Low impact toughness and brittle failure was attributed to the hard martensitic structure in the weld zone. Upon PWHT-1, the impact toughness improved to 59 ± 2 J which is due to the tempering of hard martensitic structure. PWHT-2 showed the major improvement in impact toughness (132 ± 2) J. The highest improvement in impact toughness was due to the softening by tempering of martensitic structure in the weld zone. In both the PWHT conditions, the impact toughness values satisfy the minimum average impact toughness as per standard EN 1559:1999 (Average impact toughness: 47 J with minimum single value as 37 J) [18] after test in as-welded and PWHT condition.

## 6. Conclusion

In this work, the efficacy of PWHT on dissimilar P92 steel-AISI 304H ASS weld joint fabricated by A-TIG welding was studied. By summarizing the above work, the mentioned conclusion can be drawn:

- The microstructure of HAZs showed different characteristics after PWHTs. After PWHT-1, the P92 steel side CGHAZ showed globular $M_{23C6}$ precipitates and fine precipitates (V/Nb rich MX type) in the CGHAZ. Whereas, in FGHAZ existed precipitates coarsened and some new precipitates were also formed. After PWHT- 2, the microstructure of P92 FGHAZ, P92 CGHAZ and weld zone were observed to be

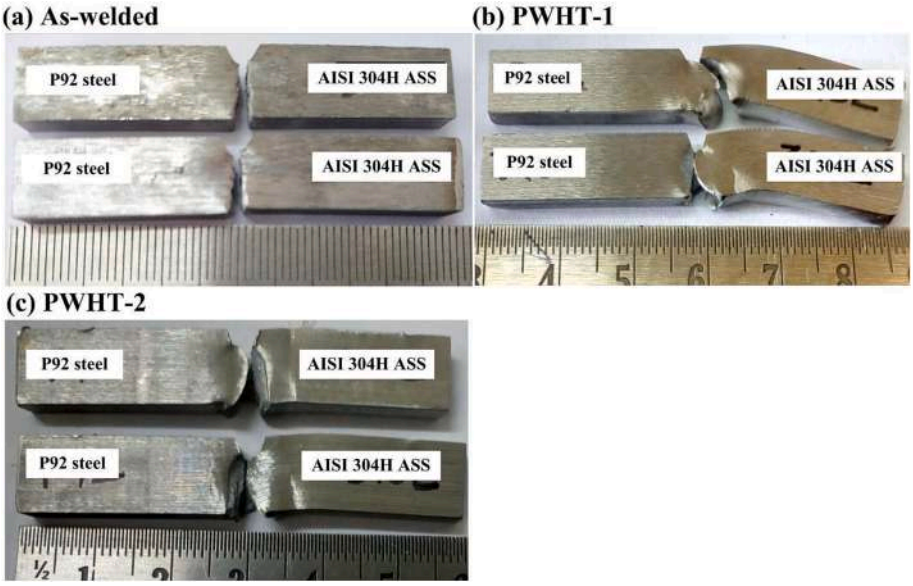


**Fig. 9.** The photographs of dissimilar P92 steel-AISI 304H ASS A-TIG weld joint impact toughness test samples.

quite similar. This could be due to the re-austenitisation during this PWHT regime.

- PWHT-1 results in the lowering of hardness of P92 steel side HAZs and weld zone in comparison to that of as- welded joint. The micro-hardness distribution curve after PWHT-2 shows almost negligible variation at P92 side and weld zone.
- In tensile testing, the failure location has changed to P92 steel base metal from AISI 304H ASS which suggests that P92 steel becomes weak after the post weld heat treatments. Also, PWHTs result in improvement in ductility (PWHT-1: 38% and PWHT-2: 45%) due to the tempering of weld zone.
- Upon PWHTs the weld zone impact toughness also improved (PWHT-1: 59 ± 2 J and PWHT-2: 132 ± 2 J) and satisfy the minimum average impact toughness as per standard EN 1559:1999.

## CRediT authorship contribution statement

**Pratishtha Sharma:** Writing – original draft, Visualization, Validation, Resources, Project administration, Methodology, Conceptualization. **Dheerendra Kumar Dwivedi:** Supervision. **Gaurav Sharma:** Writing – original draft, Data curation.

## Declaration of Competing Interest

The authors declare the following financial interests/personal relationships which may be considered as potential competing interests: [Dr. Pratishtha Sharma reports administrative support, article publishing charges, and writing assistance were provided by ABES Engineering College, Ghaziabad.].

## Data availability

Data will be made available on request.

## References

[1] L. Maddi, G.S. Deshmukh, A.R. Ballal, D.R. Peshwe, R.K. Paretkar, K. Laha, et al., Effect of Laves phase on the creep rupture properties of P92 steel, Mater. Sci. Eng. A 668 (2016) 215–223, https://doi.org/10.1016/j.msea.2016.05.074.
[2] Y. Zhou, Y. Liu, X. Zhou, C. Liu, J. Yu, Y. Huang, et al., Precipitation and hot deformation behavior of austenitic heat-resistant steels: A review, J. Mater. Sci. Technol. 33 (2017) 1448–1456, https://doi.org/10.1016/j.jmst.2017.01.025.
[3] P. Sharma, D.K. Dwivedi, Improving the strength-ductility synergy and impact toughness of dissimilar martensitic-austenitic steel joints by A-TIG welding with wire feed, Mater. Lett. 285 (2020) 2–5, https://doi.org/10.1016/j.matlet.2020.129063.
[4] P. Sharma, D.K. Dwivedi, A-TIG welding of dissimilar P92 steel and 304H austenitic stainless steel: Mechanisms, microstructure and mechanical properties, J. Manuf. Process. 44 (2019) 166–178.
[5] P. Sharma, D.K. Dwivedi, Study of flux assisted-tungsten inert gas welding of bimetallic P92 martensitic steel-304H austenitic stainless steel using $SiO_2$-$TiO_2$ binary flux, Int. J. Pressure Vessels Piping (2021) 104423, https://doi.org/10.1016/j.ijpvp.2021.104423.
[6] A. Kulkarni, D.K. Dwivedi, Dissimilar metal welding of P91 steel-AISI 316L SS with Incoloy 800 and Inconel 600 interlayers by using activated TIG welding process and its effect on the microstructure and mechanical properties, J. Mater. Process. Technol. 274 (2019) 1–14, https://doi.org/10.1016/j.jmatprotec.2019.116280.
[7] R.S. Yidyarthy, A. Kulkarni, D.K. Dwivedi, Study of microstructure and mechanical property relationships of A-TIG welded P91–316L dissimilar steel joint, Mater. Sci. Eng. A 695 (2017) 249–257, https://doi.org/10.1016/j.msea.2017.04.038.
[8] P. Sharma, D.K. Dwivedi, Wire - feed assisted A - TIG welding of dissimilar steels, Arch. Civ. Mech. Eng. 1 (2021) 81, https://doi.org/10.1007/s43452-021-00235-1.
[9] B. Arivazhagan, M. Vasudevan, A Study of Microstructure and Mechanical Properties of Grade 91 Steel A-TIG, Weld Joint 22 (2013) 3708–3716, https://doi.org/10.1007/s11665-013-0694-9.
[10] N. Saini, R.S. Mulik, M. Mohan, Influence of filler metals and PWHT regime on the microstructure and mechanical property relationships of CSEF steels dissimilar welded joints, Int. J. Pressure Vessel Piping 170 (2019) 1–9, https://doi.org/10.1016/j.ijpvp.2019.01.005.
[11] C. Pandey, M. Mohan, P. Kumar, Softening mechanism of P91 steel weldment using heat treatments, Arch. Civ. Mech. Eng. 9 (2019) 297–310, https://doi.org/10.1016/j.acme.2018.10.005.
[12] J. Cao, Y. Gong, Z.G. Yang, Microstructural analysis on creep properties of dissimilar materials joints between T92 martensitic and HR3C austenitic steels, Mater. Sci. Eng. A 528 (2011) 6103–6111, https://doi.org/10.1016/j.msea.2011.04.057.
[13] G. Chen, Q. Zhang, J. Liu, J. Wang, X. Yu, J. Hua, et al., Microstructures and mechanical properties of T92/Super304H dissimilar steel weld joints after high-temperature ageing, Mater. Des. 44 (2013) 469–475, https://doi.org/10.1016/j.matdes.2012.08.022.
[14] J. Cao, Y. Gong, Z. Yang, X. Luo, F. Gu, Z. Hu, Creep fracture behavior of dissimilar weld joints between T92 martensitic and HR3C austenitic steels, Int. J. Pressure Vessel Piping 88 (2011) 94–98, https://doi.org/10.1016/j.ijpvp.2011.01.003.
[15] C. Pandey, M. Mohan, P. Kumar, N. Saini, A Comparative study of autogenous tungsten inert gas welding and tungsten arc welding with filler wire for dissimilar P91 and P92 steel weld joint, Mater. Sci. Eng. A 712 (2018) 720–737, https://doi.org/10.1016/j.msea.2017.12.039.
[16] Wi-Geol Seo, Effect of post-weld heat treatment on the microstructure and hardness of P92 steel in IN740H/P92 dissimilar weld joints, Mater. Characterization 160 (2020) 110083, https://doi.org/10.1016/j.matchar.2019.110083.
[17] J. Cao, Y. Gong, K. Zhu, Z. Yang, X. Luo, F. Gu, Microstructure and mechanical properties of dissimilar materials joints between T92 martensitic and S304H austenitic steels, Mater. Des. 32 (2011) 2763–2770, https://doi.org/10.1016/j.matdes.2011.01.008.
[18] V. Maduraimuthu, M. Vasudevan, P. Parameswaran, Studies on improvement of toughness in modified 9Cr-1Mo steel A-TIG weld joint, Trans. Indian Inst. Metals. 68 (2015) 181–189, https://doi.org/10.1007/s12666- 014-0456-x.